Available online at http://scik.org

Commun. Math. Biol. Neurosci. 2022, 2022:57

https://doi.org/10.28919/cmbn/7500

ISSN: 2052-2541

# THE DYNAMICS OF THE SEIR EPIDEMIC MODEL UNDER THE INFLUENCE OF DELAY

REEM MUDAR HUSSIEN[1], RAID KAMEL NAJI[2,*]

[1]Department of Civil Engineering, Al-Farabi University College, Iraq

[2]Department of Mathematics, University of Baghdad, College of Science, Iraq



**Abstract:** An SEIR delayed epidemic model with nonlinear incidence and treatment rates is proposed and investigated. There is a realistic zone where the model's solutions are non-negative and bounded for all time. The stability of the two equilibrium points is explored both locally and globally. The stability and direction of Hopf-bifurcation are established using the normal form and center manifold reduction of the system. Finally, a numerical simulation to back up our analytical findings is used. The system has at most two equilibrium points, and when the delay surpasses a certain value, it exhibits a Hopf bifurcation.

**Keywords:** time delay, media coverage, nonlinear incidence and treatment rates, stability, Hopf Bifurcation.

**2010 AMS Subject Classification:** 92D30, 34C23, 34D20.

## 1. INTRODUCTION

Infectious disease mathematical modeling is a potent and extensively used approach for predicting infection, lethality, and mortality rates in a certain country or around the world, see for example

*Corresponding author

E-mail address: rknaji@gmail.com

Received May 16, 2022

[1-3] and the references therein. It may also indicate the most effective administrative procedures and social containment measures for minimizing loss of life and productivity while also limiting the spread of the disease. The SIR technique (Susceptible, Infected, and Recovered) proposed by Kermack and McKendrick in 1927 is a popular method for developing epidemiological models [4]. It has been frequently used to simulate the COVID-19 epidemic's spread, control measures, and economic output in many countries. SIR models, for example, can be simply expanded to encompass other features of the disease [5-6]. In Banerjee et al., [7], for example, incorporating viral load and its impact on the defensive human system into the SIR model allowed for the identification of potential reasons for epidemic two-phase exponential growth. Another natural extension is to consider the virus's incubation time. SEIR-models are the most common name for such models, where *E* stands for exposed [8]. Theoretical studies of several facets of the recent SARS-CoV-2 pandemic used SEIR models extensively. Such models were utilized in particular to evaluate the influence of various lockdown intensities on epidemic propagation [9-10]. Chinazzi et al [11] used the SEIR model to evaluate the influence of domestic and international travel restrictions on the COVID-19 outbreak's spread.

On the other hand, the latent period can range from days to years, as in influenza A H1N1 [12]. The generation time, which is defined as the time between a patient becoming infected and infecting another case [13], is influenced by the latent period. Particular focus has recently been dedicated to investigating specific diseases and taking into account incubation period, recovery time, isolation, and other aspects [14-16]. When epidemics spread, there are various kinds of delays, including immunization period delays, infectious period delays, and incubation period delays. The constant delay in [17] indicates the constant infectious period after which the infected persons are removed, whereas the constant delay in [18] represents the constant latency time, which is the time after which the infected individuals are removed.

It is generally understood in the study of infectious disease transmission that transmission of infection progress plays a crucial role in epidemic behavior; that is, differing incidence rates can change the system's behavior. The number of infectives increases linearly in the bilinear incidence

rate, which is accurate for a small population of infected persons but unrealistic for a high number of infectives. As a result, a number of studies [1, 6, 19] have focused on nonlinear incidence rates in disease transmission dynamics. Based on the values of $q_1$ and $q_2$, there are three types of incidence functions $g(I) = \frac{I^{q_1}}{1+dI^{q_2}}$. For example, Xiao and Ruan [20] used a nonmonotone incidence rate with $q_1 = 1$ and $q_2 = 2$ to reflect the psychological effect. A saturated incidence rate is considered with $q_1 = q_2 = 2$ by Ruan and Wang in [21]. The incidence functions $g(I)$ may be influenced by factors such as media coverage, population density, and lifestyle [6, 22-26]. It's worth emphasizing that media coverage is critical in aiding both government officials and individuals in responding to the disease [25]. A number of mathematical models have also been constructed to describe the impact of media coverage on infectious disease transmission patterns. Sun et al. [26] investigated the effects of media coverage on transmission dynamics using a nonlinear function of the number of infective people $g(I) = \beta_1 + \frac{\beta_2 I}{m+I}$ in their transmission term. Treatment is widely established for healing sickness and reducing the spread of resistant pathogens, and in conventional epidemic models, it is assumed to be either constant or proportional to the number of infected individuals. Wang and Ruan [27] proposed a SIR epidemic model with a constant treatment rate.

$$T(I) = \begin{cases} r, & I > 0 \\ 0, & I = 0 \end{cases}$$

where $r$ is a positive constant. Further, Zhou and Fan [28] modified the treatment rate to Holling type II as given by:

$$T(I) = \frac{\beta I}{1+\gamma I}, \ I \geq 0, \ \gamma > 0, \ \beta > 0$$

In addition, Dubey et al. [29] converted the treatment rate to a Holling type III functional for use in a susceptible–exposed–infectious–recovered (SEIR) model to describe the treatment of a reemerging illness with existing treatment modalities, with the following form:

$$T(I) = \frac{aI^2}{1+bI^2}, \ I \geq 0, \ a > 0, \ b > 0.$$

In light of the foregoing, the purpose of this paper is to develop and analyze a delayed SEIR epidemic model that includes the effects of media coverage on disease transmission using a

nonlinear Monod–Haldane incidence rate, as well as to investigate the effects of a Holling type III treatment rate on infection disease. A time delay owing to the incubation period is also used within a nonlinear Monod- Haldane incidence rate.

The paper is organized as follows: In section 2, a mathematical model formulation is established. In section 3, the positivity and boundedness of the solutions are discussed. In section 4, the possible equilibrium points and the basic reproduction number are determined. Moreover, in sections 5 and 6, the local and global dynamics of the system are studied. In section 7, the conditions of Hopf bifurcation occurrence are established. In section 8, the properties of Hopf bifurcation are investigated. In section 9, numerical simulation illustrates the main theoretical results and a brief discussion. Finally, the obtained results are discussed in section 10.

## 2. THE MODEL FORMULATION

A mathematical epidemic model of the $SEIR$ type with nonlinear incidence and treatment rates is proposed and studied. The entire constant population, which is denoted by $N$, is separated into four disjoint compartments so that $N = S(t) + E(t) + I(t) + R(t)$, where $S(t)$ stands for susceptible individuals; $E(t)$ stands for exposed individuals who have been infected and take $\tau$ to become infectious; $I(t)$ stands for infectious individuals; $R(t)$ stands for removed individuals who cannot return to the susceptible class because they have been quarantined or have acquired permanent immunity. The model considers three explicit functional types rates, which are explained below:

1. The nonlinear Monod–Haldane functional-type incidence rate is represented by the term $F_1(S,I) = g_1(I)SI = \frac{\beta_1}{1+\alpha I^2}SI$, where $\beta_1$ is the measure of the force of infection and $\alpha$ reports the down-regulation or psychological effect on the infection rate when $I$ becomes large.
2. The expression $F_2(S,I) = g_2(I)SI = \frac{\beta_2 SI^2}{m+I}$ refers to the lower value of the contact rate when infectious people are reported. Clearly, as the number of infected people grows uncontrolled, the term $g_2(I)$ approaches its maximum, which is indicated by $\beta_2$. When the reported

infective number reaches $m$, which stands for the nonresponse rate of individuals to media notifications, it equals half of the maximum $\beta_2$. Finally, because the media alarm report can't totally stop the disease from spreading, it's believed that $\beta_1 \geq \beta_2$.

3. The Holling type III treatment rate is represented by the formula $F_3(I) = \frac{aI^2}{1+bI^2}$, where $a$ and $b$ are both nonnegative constants that reflect the cure rate of infected persons, and the limitation rate of treatment availability, respectively. The Holling type III treatment rate describes a situation in which the removal rate increases rapidly at first due to an increase in infective individuals, then gradually decreases until it reaches a saturation point. Any increase in infective individuals after then will have no effect on the elimination rate.

The following assumptions describe the interaction among the above four classes:

- The susceptible population grows as the recruitment rate $\Lambda$ rises, and declines as a result of direct contact with infectious people, as indicated by $F(S,I) = F_1(S,I) - F_2(S,I)$ and the natural death rate $\mu$ of all human classes.
- The disease is transmitted by contact between the individuals in the $S$ compartment and $I$ compartment according to the nonlinear transmission rate $g_1(I) - g_2(I) = \left(\frac{\beta_1}{1+\alpha I^2} - \frac{\beta_2 I}{m+I}\right)$.
- With a transmission rate of $g_1(I) - g_2(I)$, the newly infected individuals from $S$ transfer to the exposed class $E$ and remain there for a given latent time $\tau$. In fact, the $E$ individuals live in the latent period $[t-\tau, t]$ with a probability of $e^{-\mu\tau}$ before becoming infected or recovering and moving into the $R$-compartment with a recovery rate of $k$.
- The infected individuals recover and move into $R$ either naturally with a $\gamma$ recovery rate or with a $F_3(I) = \frac{aI^2}{1+bI^2}$ treatment rate.

As a result of the stated assumptions, the mathematical model that describes the dynamics of the $SEIR$ model, as shown in the block diagram in Fig. 1, can be built as follows.

$$\begin{aligned}
\frac{dS}{dT} &= \Lambda - F(S,I) - \mu S,\\
\frac{dE}{dT} &= F(S,I) - F\big(S(t-\tau),I(t-\tau)\big)\ e^{-\mu\tau} - (\mu+k)E,\\
\frac{dI}{dT} &= F(S(t-\tau),I(t-\tau))\ e^{-\mu\tau} - (\mu+\gamma)I - F_3(I),\\
\frac{dR}{dT} &= F_3(I) + \gamma I - \mu R + kE.
\end{aligned} \tag{1}$$

We may deduce from the preceding system that $S$, $E$, and $I$ are not affected by $R$. Thus, it is sufficient to consider the following reduced system for the study, and then solve the $R$ equation independently of the system using the obtained values of $I$, and $E$.

$$\begin{aligned}
\frac{dS}{dT} &= \Lambda - F(S,I) - \mu S,\\
\frac{dE}{dT} &= F(S,I) - F\big(S(t-\tau),I(t-\tau)\big)\ e^{-\mu\tau} - (\mu+k)E,\\
\frac{dI}{dT} &= F(S(t-\tau),I(t-\tau))\ e^{-\mu\tau} - (\mu+\gamma)I - F_3(I).
\end{aligned} \tag{2}$$

The initial condition of the system (2) is given by $S(\theta) = \Phi_1(\theta)$, $E(\theta) = \Phi_2(\theta)$, $I(\theta) = \Phi_3(\theta)$, with $\Phi = [\Phi_1, \Phi_2, \Phi_3] \in C$ such that $\Phi_i(\theta) \geq 0$, $i = 1,2,3$ for $\theta \in [-\tau, 0]$, $\Phi_i(0) > 0$, $i = 1,2,3$, where $C$ denotes the Banach space of continuous function mapping the interval $[-\tau, 0]$ into $\mathbb{R}^3_+ = \{(S,E,I); S \geq 0, E \geq 0, I \geq 0\}$.

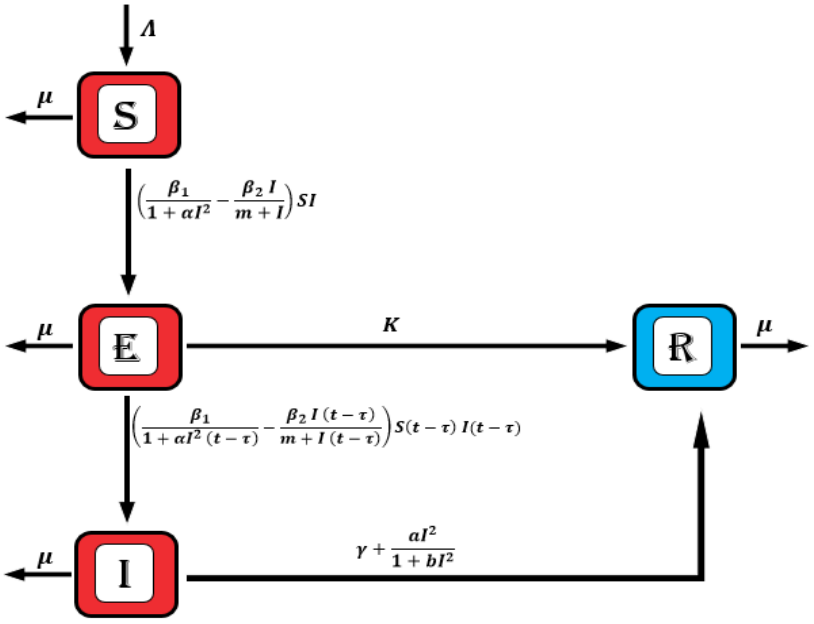


**Figure 1**: *The chart for the delayed system (1).*

## 3. POSITIVITY AND BOUNDEDNESS OF THE SOLUTIONS

The system (2) keeps track of the population dynamics in each of the susceptible and infected compartments. As a result, it's essential to demonstrate that all state variables with nonnegative initial conditions will remain positive and bounded for the rest of their lives. As a result, the following theorem looks at the system's positivity and boundedness.

**Theorem 1.** For all $t \geq 0$, all state variables of the system (2) remain non-negative and bounded.

***Proof***. First, the positivity of all solutions of system (2) is shown for $t \geq 0$.

From, the first equation of system (2) we have for $t \geq 0$

$$\frac{dS}{dt} \geq -S\left[\left(\frac{\beta_1}{1+\alpha I^2} - \frac{\beta_2 I}{m+I}\right) I + \mu\right].$$

By solving this inequality it is obtained that:

$$S(t) \geq S(0)\, exp - \left\{\int_0^t \left[\left(\frac{\beta_1}{1+\alpha I^2(\in)} - \frac{\beta_2 I(\in)}{m+I(\in)}\right) I(\in) + \mu\right] d \in\right\}.$$

Since $S(0) > 0$, we get $S(t) > 0$ for all $t \geq 0$.

Now, the positivity of $I(t)$ is shown, from the infected equation it is observed that:

$$\frac{dI}{dt} = I\left[\left(\frac{\beta_1}{(1+\alpha I^2(t-\tau))I(t)} - \frac{\beta_2}{(m+I(t-\tau))I(t)}\right) e^{-\mu\tau}\, S(t-\tau)\, I(t-\tau) - (\mu+\gamma) - \frac{aI}{1+bI^2}\right].$$

This gives:

$$I(t) = I(0)\, exp\left\{\left[\int_0^t \left(\frac{\beta_1}{(1+\alpha I^2(\in -\tau))I(\in)} - \frac{\beta_2}{(m+I(\in))}\right) e^{-\mu\tau} S(\in -\tau) I(\in -\tau) - \frac{aI(\in)}{1+bI^2(\in)} - (\mu+\gamma)\right] d(\in)\right\}.$$

Similarly, this implies that for all $t \geq 0$, we have $I(t) > 0$.

In the same manner, the proof of $E(t) > 0$ for all $t \geq 0$ can be done

Next, the proof of the boundedness of the solutions of system (2) for all $t \geq 0$, is given below:

$$N(t) = S(t) + E(t) + I(t).$$

Then, the following is obtained:

$$\frac{dN}{dt} = \Lambda - \mu N - \left(\gamma + \frac{aI}{1+bI}\right) I - kE,$$

which gives that:

$$\frac{dN}{dt} \leq \Lambda - \mu N$$

So, by Granwall Lemma, it is observed that:

$$N(t) \leq N(0)\, e^{-\mu t} \; + \frac{\Lambda}{\mu}(1 - e^{-\mu t}),$$

which yields that

$$\lim_{t \to +\infty} \; sup \; N(t) \; \leq \frac{\Lambda}{\mu}.$$

Furthermore, $\frac{dN}{dt} < 0$, if $N > \frac{\Lambda}{\mu}$.

Thus, the invariant region of the solution is $0 < \lim_{t \to +\infty}(S(t) + E(t) + I(t)) \leq \frac{\Lambda}{\mu}$.

This implies the boundedness of $N(t)$.

## 4. THE EXISTENCE OF EQUILIBRIUM POINTS AND THE BASIC REPRODUCTION NUMBER

For the existence of equilibrium points, the righthand side terms of the model (2) are set to zero, with $F(S, I)$, and $F_3(I)$ are always positive, continuously differentiable, and monotonically rising for all $S > 0$ and $I > 0$. That is, they meet the following requirements:

$\boldsymbol{\mathcal{H}_1}$: $F(S, I) > 0$, $F'_S(S, I) > 0$, $F'_I(S, I) > 0$ for all $S > 0$, and $I > 0$.

$\boldsymbol{\mathcal{H}_2}$: $F(S, 0) = F(0, I) = F'_S(S, 0) = 0$, $F'_I(S, 0) > 0$ for all $S > 0$, and $I > 0$.

$\boldsymbol{\mathcal{H}_3}$: $F_3(0) = 0$, $F'_3(I) > 0$ for all $I > 0$.

As a result, the model (2) has two equilibrium points described below:

1. Disease-free equilibrium point (DFEP) that denoted by $Q_0(S_0, 0,0)$, where $S_0 = \frac{\Lambda}{\mu}$ is always existed and represented the eradication of infectious individuals.

Furthermore, it is well known that the basic reproduction number is used to assess a disease's transmission potential. It's the average number of secondary infections caused by a normal infection in a population where everyone is vulnerable, and it's calculated using the disease-free equilibrium point. As a result, the fundamental reproduction number is computed as follows: Consider the Jacobian matrix of infected compartments in the model (2) at $Q_0$ that can be written as:

$$J_{DFE} = \begin{bmatrix} -(\mu + k) & \beta_1 S_0 - \beta_1 S_0\ e^{-\mu\tau} \\ 0 & \beta_1 S_0\ e^{-\mu\tau} - (\mu + \gamma) \end{bmatrix}.$$

As a result, the linearized form of the infected compartments equations for the system (2) at $Q_0$ can be rewritten as:

$$\frac{d}{dt}X(t) = \mu_1\, X(t-\tau) - \mu_2\, X(t), \tag{3}$$

where:

$$X(t) = \begin{bmatrix} E(t) \\ I(t) \end{bmatrix},$$

with:

$$\mu_1 = \begin{bmatrix} 0 & -\beta_1 S_0\ e^{-\mu\tau} \\ 0 & \beta_1 S_0\ e^{-\mu\tau} \end{bmatrix},\ \mu_2 = \begin{bmatrix} (\mu + k) & -\beta_1 S_0 \\ 0 & (\mu + \gamma) \end{bmatrix}.$$

Let $y_0 = (y_1, y_2)^T$ be the initial values for number of individuals in the compartments $E(t)$ and $I(t)$ at $t = 0,$ then from the above equation the distribution of the remaining population of the compartments $E(t)$ and $I(t)$ at time $t > 0$ is $y(t) = e^{-\mu_2 t}\ y_0$. Then the total number of newly infected individuals is:

$$\bar{y} = \int_{\tau}^{\infty} \mu_1 y(t-\tau)dt = \mu_1\ \mu_2^{-1}\ y_0.$$

Now since the matrix $\mu_2$, is nonsingular then

$$\mu_1\mu_2^{-1} = \begin{bmatrix} 0 & \frac{-\beta_1 S_0\ e^{-\mu\tau}}{(\mu+\gamma)} \\ 0 & \frac{\beta_1 S_0\ e^{-\mu\tau}}{(\mu+\gamma)} \end{bmatrix}$$

Therefore, the reproduction number for system $(2)$ is the spectral radius of the matrix $(\mu_1\mu_2^{-1})$, which is given by, $R_0 = \frac{\beta_1 S_0\ e^{-\mu\tau}}{(\mu+\gamma)}$.

Biologically, the term $\frac{1}{(\mu+\gamma)}$ is the time spent as an infections individual, while $e^{-\mu\tau}$ is the survival rate of infected individual in latent period. Hence the basic reproduction number $R_0$ gives the number of secondary infections of susceptible individuals that one infected individual can produce in a disease-free population $S_0$.

2. The endemic equilibrium point (EEP) that represented by $Q^*(S^*, I^*, E^*)$, where $S^*$ and $I^*$ satisfy the following equations.

$$\Lambda - \mu S = F(S, I). \tag{4}$$

$$F(S, I) = e^{\mu\tau}\big((\mu + \gamma)I + F_3(I)\big). \tag{5}$$

By substituting the expression of $S$ by $I$, we obtain the following equation for $I$:

$$G(I) = F\left(\frac{\Lambda - e^{\mu\tau}\big((\mu+\gamma)I + F_3(I)\big)}{\mu}, I\right) - e^{\mu\tau}\big((\mu + \gamma)I + F_3(I)\big).$$

Clearly, $G(0) = 0$. Also, there exists a positive $I_0$ such that $\Lambda = e^{\mu\tau}\big((\mu + \gamma)I_0 + F_3(I_0)\big)$. Thus

$$G(I_0) = F(0, I_0) - \Lambda = -\Lambda < 0. \tag{6}$$

Furthermore, when $I \geq 0$, then it is obtained, due to the continuously differentiable of $G(I)$, that:

$$\begin{aligned} G'(0) &= \lim_{I \to 0^+} \frac{G(I) - G(0)}{I - 0} \\ &= F_I'(S_0, 0) - e^{\mu\tau}\big(\mu + \gamma + F_3'(0)\big)F_S'(S_0, 0) - e^{\mu\tau}\big(\mu + \gamma + F_3'(0)\big) \\ &= F_I'(S_0, 0) - e^{\mu\tau}\big(\mu + \gamma + F_3'(0)\big) = e^{\mu\tau}\big(\mu + \gamma + F_3'(0)\big)(R_0 - 1). \end{aligned}$$

Thus, the value of $R_0 > 1$ ensures that $G'(0) > 0$. And $G(I)$ is continuous on $[0, I_0]$, then there exists some $I^* \in (0, I_0)$ such that $G(I^*) = 0$. Since $F_3(I)$ is strictly monotonically increasing, It is obtained that

$$e^{\mu\tau}\big((\mu + \gamma)I^* + F_3(I^*)\big) < e^{\mu\tau}\big((\mu + \gamma)I_0 + F_3(I_0)\big).$$

Therefore, $S^* = \frac{\Lambda - e^{\mu\tau}\big((\mu+\gamma)I^* + F_3(I^*)\big)}{\mu} > 0$ and then $E^* > 0$, then we have proved the existence of EEP for model (2) under condition $R_0 > 1$.

## 5. STABILITY OF DFEP

In this section, the stability of $Q_0$ is established as shown in the following theorems

**Theorem 2.** The DFEP of the system (2) is

1. Asymptotically stable if $R_0 < 1$.
2. Unstable if $R_0 > 1$.

**Proof.** According to the linearization technique, the Jacobian of the system (2) at the $Q_0$ is written as:

$$J_{Q_0} = \begin{bmatrix} -\mu & 0 & -\beta_1 S_0 \\ 0 & -(\mu+k) & \beta_1 S_0 \left(1 - e^{-(\mu+\lambda)\tau}\right) \\ 0 & 0 & \beta_1 S_0 \; e^{-(\mu+\lambda)\tau} - (\mu+\gamma) \end{bmatrix}$$

Therefore, the eigenvalues can be written $\lambda_1 = -\mu \; and \; \lambda_2 = -(\mu + k)$, which are negative roots, while the third root that specifies the stability type for $Q_0$ can be obtained by,

$$\lambda_3 = \beta_1 S_0 \; e^{-(\mu+\lambda)\tau} - (\mu+\gamma).$$

Now, let $f(\lambda) = \lambda - \beta_1 S_0 \; e^{-(\mu+\lambda)\tau} + (\mu+\gamma)$, thus:

1. If $R_0 > 1$, it can be seen that, for real $\lambda$, the following is observed:

$f(0) = (\mu+\gamma)[1 - R_0] < 0$, and as $\lambda \longrightarrow \infty$, then $f(\lambda) = \infty$.

Hence, if $R_0 > 1$, there exists at least one positive root of $f(\lambda) = 0$, and that makes $Q_0$ unstable.

2. If $R_0 < 1$, it is assumed that $\lambda = \alpha + i\beta$, where $\alpha = \beta_1 S_0 \; e^{-(\mu+\alpha)} \cos(\tau\,\beta) - (\mu+\gamma)$, thus: for $\alpha \geq 0$, it is observed that $\alpha \leq \beta_1 S_0 \; e^{-\mu\tau} - (\mu+\gamma)$.

Hence it is obtained that $\alpha \leq (\mu+\gamma)(R_0 - 1)$, which gives a contradiction due to the negativity of the right-hand side of the last inequality, so $\alpha < 0$. Therefore, the disease-free equilibrium of system (2) is locally asymptotically stable, otherwise is unstable.

**Theorem 3.** The DFEP that is given by $\mathrm{Q_0} = \left(\frac{\Lambda}{\mu}, 0, 0\right)$ of the system (2) is globally asymptotically stable if and only if $\mathrm{R_0} \leq 1$.

**Proof.** Consider the Lyapunov function $W(t) = \sum_{i=1}^{n} W_i(t)$, where

$$W_1(t) = \int_{s_0}^{s(t)} \left(1 - \frac{k(s_0)}{k(s)}\right) ds,$$

$$W_2(t) = \int_0^{\tau} y\big(s(t-\theta), I(t-\theta)\big) e^{-\mu\theta} \frac{k(s_0)}{k\big(s(t-\theta)\big)} d\theta,$$

$$W_3(t) = I(t),$$

$$W_4(t) = E(t),$$

with $k(s) = \frac{F(S,I)}{I}$. Thus it is obtained that:

$$\frac{dW}{dt} = -\mu(s - s_0)\left(1 - \frac{k(s_0)}{k(s)}\right) + \left(y\big(s(t-\tau), I(t-\tau)\big)\right) e^{-\mu\tau} \frac{k(s_0)}{k\big(s(t-\tau)\big)} - (\mu+\gamma)I - \frac{aI^2}{1+bI^2} - (\mu+k)E.$$

Furthermore, according to the conditions $\mathcal{H}_1, \mathcal{H}_2$, it is observed that

$-\mu(s(t)-s_0)\left(1-\frac{k(s_0)}{k(s)}\right)\leq 0$, with equality if and only if $s(t)=s_0$.

Now, since

$$y\big(s(t-\tau),I(t-\tau)\big)e^{-\mu\tau}\frac{k(s_0)}{k\big(s(t-\tau)\big)}-(\mu+\gamma)I$$
$$=(\mu+\gamma)I\left[\frac{y\big(s(t-\tau),I(t-\tau)\big)}{(\mu+\gamma)I}e^{-\mu\tau}\frac{k(s_0)}{k\big(s(t-\tau)\big)}-1\right].$$

Then, according to the condition $\mathcal{H}_3$, it is obtained that

$$(\mu+\gamma)I\left[e^{-\mu\tau}\frac{k(s_0)}{(\mu+\gamma)}-1\right]\Rightarrow(\mu+\gamma)I[R_0-1]$$

Therefore, $R_0\leq 1$ yield $\frac{dW}{dt}\leq 0,\forall t>0$, where $\frac{dW}{dt}=0$ holds if $s=s_0$, $I=0$, and $E=0$. Hence $Q_0$ is globally asymptotically stable.

## 6. Stability Of EEP

The stability around EEP is investigated in this section as presented in the following theorems.

**Theorem 4** For any $\tau\geq 0$, the EEP of the system (2) is locally asymptotically stable if the following conditions are met.

$$(b_2)^2+((\mu+\gamma)+a_4)^2>(b_1)^2. \tag{7}$$
$$(b_2)^2((\mu+\gamma)+a_4)^2>\mu^2(b_1)^2. \tag{8}$$

**Proof**. From the linearization technique, the Jacobian matrix of the system (2) at $Q^*$ can be written as:

$$J_{Q^*}=\begin{bmatrix}-b_2 & 0 & -b_1\ e^{\mu\tau}\\ (b_2-\mu)\big(1-e^{-(\mu+\lambda)\tau}\big) & -(\mu+k) & b_1\big(e^{\mu\tau}-e^{-\lambda\tau}\big)\\ (b_2-\mu)e^{-(\mu+\lambda)\tau} & 0 & b_1e^{-\lambda\tau}-(\mu+\gamma)-a_4\end{bmatrix},$$

where

$$b_1=(a_2-a_3a_5)e^{-\mu\tau};\ b_2=(a_1-a_3)+\mu$$
$$a_1=\frac{\beta_1I^*}{1+\alpha I^{*2}};\ a_2=\frac{\beta_1S^*(1-\alpha I^{*2})}{(1+\alpha I^{*2})^2};\ a_3=\frac{\beta_2I^{*2}}{m+I^*}$$
$$a_4=\frac{2aI^*}{1+bI^{*2}};\ a_5=\frac{(2m+I^*)s^*}{(m+I^*)I^*}\ ,\quad \text{are positive.}$$

Clearly, $\lambda_1=-(\mu+k)<0$, and the other two eigenvalues represent the roots of the following

equation

$$\lambda^2 + \left(C_1 - b_1 e^{-\lambda\tau}\right)\lambda + C_2 - b_1\ \mu e^{-\lambda\tau} = 0. \tag{9}$$

where

$$C_1 = b_2 + (\mu + \gamma) + a_4$$

$$C_2 = b_2\big((\mu + \gamma) + a_4\big)$$

Thus,

1. If $\tau = 0$, so by the Hurwitz criterion the equation (9) has two negative roots. Hence the EEP is locally asymptotically stable.
2. For $\tau > 0$, if $Q^*$ is unstable for a specific value $\tau_0$, then the roots of equation (9) must intersect the imaginary axis [21]. Now by contradiction, let $\lambda = i\theta,\ \theta > 0$ is the root of equation (9) and separating real and imaginary parts, we get

$$-b_1\theta\ \sin(\theta\tau) - \mu b_1\ \cos(\theta\tau) = \theta^2 - C_2. \tag{10}$$

$$-b_1\theta\ \cos(\theta\tau) + \mu b_1\ \sin(\theta\tau) = C_1\theta. \tag{11}$$

Furthermore, squaring and adding both sides of the above equations leads to

$$\theta^4 + (C_1^2 - 2C_2 - b_1^2)\theta^2 + C_2^2 - \mu^2 b_1^2 = 0. \tag{12}$$

Put $\theta^2 = Z$, then the last equation becomes:

$$Z^2 + A_1 Z + A_2 = 0, \tag{13}$$

where $A_1 = C_1^2 - 2C_2 - b_1^2\ ;\ A_2 = C_2^2 - \mu^2 b_1^2$.

Thus, according to conditions (7, 8) the last equation has two negative real part roots. Hence $Q^*$ is a locally asymptotically stable.

Now, the global stability of $Q^*(S^*, E^*, I^*)$ of the system (2) is studied using the Lyapunov direct method. For this objective, the following hypotheses are suggested:

$\boldsymbol{\mathcal{H}_4}$: $\frac{G(I)}{G(I^*)} \leqslant \frac{I}{I^*}\ \ for\ \ I \in (0, I^*),\ \frac{G(I)}{G(I^*)} \geqslant \frac{I}{I^*}\ \ for\ \ I \geqslant I^*.$

$\boldsymbol{\mathcal{H}_5}$: $y(s^*, I^*) \leqslant y(s(t-\tau), I(t-\tau))\ e^{-\mu\tau}$

$\boldsymbol{\mathcal{H}_6}$: $\frac{y(s(t-\tau), I(t-\tau))\ e^{-\mu\tau}}{\frac{E}{E^*} - 1} \leqslant y(s, I) \leqslant y(s, I^*).$

**Theorem 5.** Suppose that conditions $\mathcal{H}_{\mathrm{i}}$, i = 1,2,4,5,6 are satisfied. Then the EEP is a global

asymptotically stable if $R_0 > 1$.

**Proof**. Consider the Lyapunov function that is given by:

$$V(t) = V_1(t) + V_2(t),$$

where

$$V_1(t) = s - s^* - \int_{s^*}^{s} \frac{y(s^*, I^*)}{y(\theta, I^*)} d\theta + E - E^* - E^* \ln \frac{E}{E^*} + I - I^* - I^* \ln \frac{I}{I^*}$$
$$-2e^{-\mu t} \int_{t-\tau}^{t} y\big(s(\theta), I(\theta)\big) e^{\mu\theta} d\theta.$$

$$V_2(t) = y(s^*, I^*) e^{-\mu t} \left( \int_{t-\tau}^{t} \frac{y(s(\theta), I(\theta)) e^{\mu\theta}}{y(s^*, I^*)} - 1 - \ln \frac{y(s(\theta), I(\theta)) e^{\mu\theta}}{y(s^*, I^*)} \right) d\theta.$$

$V(t)$ is defined and continuously differentiable for all positive values of $S(t)$, $E(t)$, and $I(t)$, with $V(0) = 0$ at $Q^*(S^*, E^*, I^*)$.

Thus, the time derivative of $V(t)$ along the solution of the system (2) is given by:

$$\frac{dV(t)}{d(t)} = \mu s^* \left(1 - \frac{s}{s^*}\right)\left(1 - \frac{y(s^*,I^*)}{y(s,I^*)}\right) + y(s^*, I^*)\left(1 - \frac{y(s^*,I^*)}{y(s,I^*)} + \frac{y(s,I)}{y(s,I^*)}\right)$$
$$+ y(s^*, I^*)\left(1 - \frac{I}{I^*} - \frac{y(s(t-\tau),I(t-\tau))e^{-\mu\tau} I^*}{y(s^*,I^*)}\right) + G(I^*)\left(\frac{G(I)}{G(I^*)} - \frac{I}{I^*}\right)\left(\frac{I^*}{I} - 1\right)$$
$$+ y(s(t-\tau), I(t-\tau)) e^{-\mu\tau}\left(1 + \frac{E^*}{E} - \frac{y(s,I)E^*}{y(s(t-\tau),I(t-\tau))e^{-\mu\tau}E}\right) - y(s,I)$$
$$-2y\big(s(t-\tau), I(t-\tau)\big)e^{-\mu\tau} + y(s^*, I^*) ln \frac{y\big(s(t-\tau),I(t-\tau)\big)e^{-\mu\tau}}{y(s,I)}.$$

Accordingly, it is obtained that

$$\frac{dV(t)}{d(t)} = \mu s^* \left(1 - \frac{s}{s^*}\right)\left(1 - \frac{y(s^*,I^*)}{y(s,I^*)}\right) + y(s^*, I^*)\left(1 - \frac{y(s^*,I^*)}{y(s,I^*)} + \ln \frac{y(s^*,I^*)}{y(s,I^*)}\right)$$
$$+ y(s^*, I^*)\left(1 - \frac{y(s(t-\tau),I(t-\tau))e^{-\mu\tau} I^*}{y(s^*,I^*)I} + ln \frac{y(s(t-\tau),I(t-\tau))e^{-\mu\tau} I^*}{y(s^*,I^*)I}\right)$$
$$+ y(s^*, I^*)\left(1 - \frac{y(s^*,I^*)I}{y(s(t-\tau),I(t-\tau))e^{-\mu\tau} I^*} + ln \frac{y(s^*,I^*)I}{y(s(t-\tau),I(t-\tau))e^{-\mu\tau} I^*}\right)$$
$$+ y(s(t-\tau), I(t-\tau)) e^{-\mu\tau}\left(1 - \frac{y(s,I)E^*}{y(s(t-\tau),I(t-\tau))e^{-\mu\tau}E} + ln \frac{y(s,I)E^*}{y(s(t-\tau),I(t-\tau))e^{-\mu\tau}E}\right)$$
$$+ y(s(t-\tau), I(t-\tau)) e^{-\mu\tau}\left(1 - \frac{y(s(t-\tau),I(t-\tau))e^{-\mu\tau}E}{y(s,I)E^*} + ln \frac{y(s(t-\tau),I(t-\tau))e^{-\mu\tau}E}{y(s,I)E^*}\right)$$
$$+ G(I^*)\left(\frac{G(I)}{G(I^*)} - \frac{I}{I^*}\right)\left(\frac{I^*}{I} - 1\right) - y(s,I) - 2y(s(t-\tau), I(t-\tau))e^{-\mu\tau}$$
$$+ y(s^*, I^*)\left(\frac{y(s,I)}{y(s,I^*)} - \frac{I}{I^*} - 1 + \frac{y(s^*,I^*)I}{y(s(t-\tau),I(t-\tau))e^{-\mu\tau} I^*}\right)$$
$$+ y(s(t-\tau), I(t-\tau)) e^{-\mu\tau}\left(\frac{E}{E^*} - 1 + \frac{y(s(t-\tau),I(t-\tau))e^{-\mu\tau}E}{y(s,I)E^*}\right)$$

The function $Y(S, I)$ is monotonically increasing for any $S > 0$, hence it is obtained that:

$$\mu s^* \left(1 - \frac{s}{s^*}\right)\left(1 - \frac{y(s^*,I^*)}{y(s,I^*)}\right) \leqslant 0. \tag{14}$$

By the properties of the function $g(x) = 1 - x + \ln(x)$, when $(x > 0)$, it is noted that the global maximum of $g(x)$ is $g(1) = 0$. Hence $g(x) \leqslant 0$, where $x > 0$, so the following inequalities hold true:

$$\left.\begin{aligned} 1 - \frac{y(s^*,I^*)}{y(s,I^*)} + \ln\frac{y(s^*,I^*)}{y(s,I^*)} &\leqslant 0 \\ 1 - \frac{y(s(t-\tau),I(t-\tau))e^{-\mu\tau}I^*}{y(s^*,I^*)I} + \ln\frac{y(s(t-\tau),I(t-\tau))e^{-\mu\tau}I^*}{y(s^*,I^*)I} &\leqslant 0 \\ 1 - \frac{y(s^*,I^*)I}{y(s(t-\tau),I(t-\tau))e^{-\mu\tau}I^*} + \ln\frac{y(s^*,I^*)I}{y(s(t-\tau),I(t-\tau))e^{-\mu\tau}I^*} &\leqslant 0 \\ 1 - \frac{y(s,I)E^*}{y(s(t-\tau),I(t-\tau))e^{-\mu\tau}E} + \ln\frac{y(s,I)E^*}{y(s(t-\tau),I(t-\tau))e^{-\mu\tau}E} &\leqslant 0 \\ 1 - \frac{y(s(t-\tau),I(t-\tau))e^{-\mu\tau}E}{y(s,I)E^*} + \ln\frac{y(s(t-\tau),I(t-\tau))e^{-\mu\tau}E}{y(s,I)E^*} &\leqslant 0 \end{aligned}\right\}. \tag{15}$$

Further, by the conditions $\mathcal{H}_i,\ i = 4,5,6$, the following inequalities hold:

$$\left.\begin{aligned} &\frac{G(I)}{G(I^*)} \leqslant \frac{I}{I^*}, for\ I \in (0,I^*), and\ \frac{G(I)}{G(I^*)} \geqslant \frac{I}{I^*}, for\ I \geqslant I^*, \\ &y(s^*,I^*)\left(\frac{y(s,I)}{y(s,I^*)} - \frac{I}{I^*} - 1 + \frac{y(s^*,I^*)I}{y\left(s(t-\tau),I(t-\tau)\right)e^{-\mu\tau}I^*}\right) \leq 0, \\ &y(s(t-\tau),I(t-\tau))e^{-\mu\tau}\left(\frac{E}{E^*} - 1 + \frac{y(s(t-\tau),I(t-\tau))e^{-\mu\tau}E}{y(s,I)E^*}\right) \leq 0 \end{aligned}\right\}. \tag{16}$$

Hence, $\frac{dV(t)}{dt} \leqslant 0$ for all $S(t)$, $E(t)$, and $I(t)$ are positive, and according to the Lyapunov LaSalle asymptotic stability theorem [30], it is obtained that $Q^*$ is globally asymptotically stable.

## 7. HOPF BIFURCATION

The existence of periodic solutions of the system (2) around the EEP is explored in this section in the sense of the Hopf bifurcation theorem, which requires the existence of a pair of complex conjugate eigenvalues that are pure imaginary at the bifurcation point with the derivative of their real parts with respect to the bifurcation parameter not vanishing.

Note that, when condition (7) holds while condition (8) is reflected ($A_2 < 0$), then equation (13) has a unique positive root, namely $\theta_0$. Therefore, there is a single pair of purely imaginary roots $\mp i\theta_0$ satisfying equation (9). From equations (10,11), we get:

$$\sin(\theta_0\tau) = \frac{C_2 - \theta_0^2 - \mu b_1 \cos(\theta_0\tau)}{b_1\theta_0},$$

$$\cos(\theta_0\tau) = \frac{\mu C_2 - (C_1+\mu)\theta_0^2}{(\theta_0^2+\mu^2)b_1}.$$

Then, $\tau_n$ corresponding to $\theta_0$ can be obtained as

$$\tau_n = \frac{1}{\theta_0}\left(\arccos\left(\frac{\mu C_2 - (C_1+\mu)\theta_0^2}{b_1(\theta_0^2+\mu^2)}\right) + 2n\pi\right), n = 0,1,2,\ldots \quad (17)$$

Define

$$\tau_0 = \min \tau_n\,,\ n \geq 0, \quad (18)$$

Therefore, the following theorem is obtained.

**Theorem 6.** The EEP of the system (2) is asymptotically stable when $\tau \in [0, \tau_0)$ and it undergoes Hopf bifurcation where $\tau = \tau_0$

**Proof**. For the $\tau \in [0, \tau_0)$ the proof follows from the previous theorem. However, for $\tau = \tau_0$, the existence of the Hopf bifurcation will be proved if we can show that $Q^*$ is conditionally stable, that is the single pair of complex conjugate eigenvalues that is pure imaginary at $\tau = \tau_0$ satisfies

$$\left[\frac{d(Re\lambda(\tau))}{d\tau}\right]_{\tau=\tau_0} \neq 0$$

Differentiating equation (9) with respect to $\tau$, using the chain rule as $\lambda$ is a function of $\tau$, we have

$$\left(2\lambda + C_1 - b_1 e^{-\lambda\tau} + (\lambda+\mu)b_1\tau e^{-\lambda\tau}\right)\frac{d\lambda}{d\tau} = -\lambda b_1 e^{-\lambda\tau}(\lambda+\mu).$$

From equation (9), it is obtained that

$$\left(\frac{d\lambda}{d\tau}\right)^{-1} = \frac{(2\lambda+C_1)}{-\lambda(\lambda^2+C_1\lambda+C_2)} + \frac{b_1}{\lambda b_1(\lambda+\mu)} - \frac{\tau}{\lambda}.$$

Therefore,

$$\begin{aligned}
\frac{d}{d\tau}(Re\lambda)|_{\lambda=i\theta_0} &= Re\left(\frac{d\lambda}{d\tau}\right)^{-1}|_{\lambda=i\theta_0} \\
&= Re\left[\frac{1}{\theta_0}\left(\frac{(2i\theta_0+C_1)}{\theta_0^2 i + C_1\theta_0 - C_2 i} + \frac{b_1}{-b_1\theta_0 + ib_1\mu} + i\tau\right)\right] \\
&= \frac{1}{\theta_0}\left(\frac{2\theta_0(\theta_0^2 - C_2) + C_1^2\theta_0 - b_1^2\theta_0}{(b_1\theta_0)^2 + (b_1\mu)^2}\right) \\
&= \frac{2\theta_0^2 + (C_1^2 - 2C_2 - b_1^2)}{(b_1\theta_0)^2 + (b_1\mu)^2}
\end{aligned}$$

Obviously, under the condition (7), we have $\frac{d}{d\tau}(Re\lambda)|_{\lambda=i\theta_0} > 0$. Therefore, the transversality condition holds true and hence Hopf bifurcation occurs at $\theta = \theta_0,\ \tau = \tau_0$.

## 8. THE DIRECTION AND STABILITY OF THE HOPF BIFURCATION

The conditions for making system $(2)$ undergoes a Hopf bifurcation near $Q^*$ at critical value $\tau = \tau_0$, are found. In this section, however, with the use of the normal form and the center manifold reduction for the functional differential equations introduced by [31] the properties of the Hopf bifurcation at $\tau = \tau_0$ are established.

**Theorem 7.**

1. Suppose that $M_2 > 0$ $(M_2 < 0)$ then the Hopf bifurcation is supercritical (subcritical) and the bifurcating periodic solutions exist for $\tau > \tau_0$ $(\tau < \tau_0)$;
2. Suppose that $\nu_2 < 0$ $(\nu_2 > 0)$ then the periodic solutions are stable (unstable);
3. Suppose that $T_2 > 0$ $(T_2 < 0)$ then the periodic solutions are increase (decrease);

where $M_2$, $\nu_2$, and $T_2$ are given below

$$\left.\begin{aligned} C_1(0) &= \frac{i}{2w_0\tau_0}\left(g_{11}\ g_{20} - 2|g_{11}|^2 - \frac{|g_{02}|^2}{3}\right) + \frac{g_{21}}{2}, \\ M_2 &= -\frac{Re\{C_1(0)\}}{Re\left\{\frac{d\lambda}{d\tau}(\tau_0)\right\}}, \\ \nu_2 &= 2Re\{C_1(0)\}, \\ T_2 &= \frac{-Im\{C_1(0)\}+M_2\ Im\left\{\frac{d\lambda}{d\tau}(\tau_0)\right\}}{w_0\tau_0}. \end{aligned}\right\} \tag{19}$$

**Proof**. Let $u_1(t) = S(t) - S^*$, $u_2(t) = E(t) - E^*$, $u_3(t) = I(t) - I^*$, and $\tau = \tau_0 + \gamma$, where $\tau_0$ is define by Eq. (18) and $\gamma \in \mathbb{R}$. Then system $(2)$ can be transformed into a functional differential equation in $C = C([-1,0], \mathbb{R}^3)$ as follows:

$$u'(t) = L_\gamma(u_t) + f(\gamma, u_t), \tag{20}$$

where

$$u(t) = (u_1(t), u_2(t), u_3(t))^T \in C = C([-1,0], \mathbb{R}^3) \quad \text{and} \quad L_\gamma : C \to \mathbb{R}^3\ ,\ \ f : \mathbb{R} \times C \to \mathbb{R}^3$$

are given by:

$$L_\gamma(\phi) = (\gamma + \tau_0)[M\phi(0) + N\phi(-1)] \tag{21}$$

and the nonlinear term is

$$f(\gamma, \phi) = (\gamma + \tau_0)\begin{pmatrix} F_1 \\ F_2 \\ F_3 \end{pmatrix}$$

where

$$M=\begin{pmatrix} f_{10}^{(1)} & 0 & f_{01}^{(1)} \\ f_{10000}^{(2)} & f_{01000}^{(2)} & f_{00100}^{(2)} \\ 0 & 0 & f_{100}^{(3)} \end{pmatrix}=\begin{bmatrix} -b_2 & 0 & -b_1\ e^{\mu\tau} \\ (b_2-\mu) & -(\mu+k) & b_1 e^{\mu\tau} \\ 0 & 0 & -(\mu+\gamma)-a_4 \end{bmatrix},$$

$$N=\begin{pmatrix} 0 & 0 & 0 \\ f_{00010}^{(2)} & 0 & f_{00001}^{(2)} \\ f_{010}^{(3)} & 0 & f_{001}^{(3)} \end{pmatrix}=\begin{bmatrix} 0 & 0 & 0 \\ -(b_2-\mu)e^{-(\mu+\lambda)\tau} & 0 & -b_1 e^{-\lambda\tau} \\ (b_2-\mu)e^{-(\mu+\lambda)\tau} & 0 & b_1 e^{-\lambda\tau} \end{bmatrix},$$

with $b_1,\ b_2$, and $a_4$ are given in the $J_{Q^*}$, while

$$F_1=\sum_{i+k\geq 2}\ \frac{1}{i!k!}\ f_{ik}^{(1)}\phi_1^i(0)\phi_3^k(0),$$

$$F_2=\sum_{i+j+k+m+n\geq 2}\frac{1}{i!j!k!m!n!}\ f_{ijkmn}^{(2)}\phi_1^i(0)\phi_2^j(0)\phi_3^k(0)\tilde{\phi}_1^m(-1)\tilde{\phi}_3^n(-1),$$

$$F_3=\sum_{k+m+n\geq 2}\ \frac{1}{k!m!n!}\ f_{kmn}^{(3)}\phi_3^k(0)\tilde{\phi}_1^m(-1)\tilde{\phi}_3^n(-1),$$

where, $\phi(\theta)=(\phi_1(\theta),\phi_2(\theta),\phi_3(\theta))\in C,-1\leq\theta\leq 0$, with

$$f_{ik}^{(1)}\phi_1^i(0)\phi_3^k(0)=\frac{\partial^{i+k}f^{(1)}}{\partial\phi_1^i\phi_3^k}\Big|_{(\phi_1,\phi_3)=(0,0)},$$

$$f_{ijkmn}^{(2)}\phi_1^i(0)\phi_2^j(0)\phi_3^k(0)\phi_1^m(-1)\phi_3^n(-1)=\frac{\partial^{i+j+k+m+n}f^{(2)}}{\partial\phi_1^i\phi_2^j\phi_3^k\tilde{\phi}_1^m\tilde{\phi}_3^n}\Big|_{(\phi_1,\phi_1,\phi_3,\tilde{\phi}_1,\tilde{\phi}_3)=(0,0,0,-1,-1)},$$

$$f_{kmn}^{(3)}\phi_3^k(0)\tilde{\phi}_1^m(-1)\tilde{\phi}_3^n(-1)=\frac{\partial^{k+m+n}f^{(3)}}{\partial\phi_3^k\tilde{\phi}_1^m\tilde{\phi}_3^n}\Big|_{(\phi_3,\tilde{\phi}_1,\tilde{\phi}_3)=(0,-1,-1)}.$$

According to the Riesz representation theorem there is a $3\times 3$ matrix function $\psi(\theta,\gamma),\theta\in[-1,0]$, such that

$$L_\gamma(\phi)=\int_{-1}^{0}d\psi(\theta,\gamma)\phi(\theta),\ \phi\in C. \tag{22}$$

In fact, It can be choose

$$\psi(\theta,\gamma)=(\gamma+\tau_0)(M\delta(\theta)-N\delta(\theta+1)), \tag{23}$$

where, $\delta$ is the Dirac delta function.

For $\phi\in \mathrm{C}([-1,0],\mathbb{R}^3)$, It is defined that

$$A(\gamma)\phi(\theta)=\begin{cases}\frac{d\phi(\theta)}{d\theta}, & \theta\in[-1,0), \\ \int_{-1}^{0}d\psi(S,\gamma)\phi(S), & \theta=0,\end{cases} \tag{24}$$

and

$$R(\gamma)\phi(\theta) = \begin{cases} 0, & \theta \in [-1,0) \\ f(\gamma,\phi), & \theta = 0. \end{cases} \tag{25}$$

Thus, system (20) is equivalent to the abstract operator differential equation

$$u'(t) = A(\gamma)\, u_t + R(\gamma)\, u_t, \tag{26}$$

where, $u_t = u(t+\theta),\ \theta \in [-1,0]$.

Now, for $\varphi \in C^1([-1,0], (\mathbb{R}^3)^*)$, the adjoint operator $A^*$ of $A(0)$ is defined as:

$$A^*\varphi(S) = \begin{cases} -\frac{d\varphi(S)}{dS}, & S \in (0,1] \\ \int_{-1}^{0} \varphi(-t) d\phi^T(t,0), & S = 0 \end{cases} \tag{27}$$

and a bilinear form

$$\langle \varphi(S), \phi(\theta) \rangle = \bar{\varphi}(0)\ \phi(0) - \int_{\theta=-1}^{0} \int_{\in=0}^{\theta} \bar{\varphi}(\in -\theta)\ d\psi(\theta)\ \phi(\in)\ d \in, \tag{28}$$

where, $\psi(\theta) = \psi(\theta, 0)$, clearly $A(0)$ and $A^*$ are adjoint operators. Thus, for $\gamma = 0$ by a simple computation, we can calculate $q(\theta) = (1, q_1, q_2)^T\ e^{iw_0\tau_0\theta}$ be the eigenvector of $A(0)$ belonging to the eigenvalue $iw_0\tau_0$ and $q^*(S) = D(1, q_1^*, q_2^*)^T\ e^{-iw_0\tau_0 S}$ is the eigenvector of $A^*$ that associated with the eigenvalue $-iw_0\tau_0$, where

$$q_1 = \frac{-f_{10000}^{(2)} - f_{00010}^{(2)}\ e^{-i\tau_0 w_0} - \left(f_{00100}^{(2)} - f_{00001}^{(2)}\ e^{-i\tau_0 w_0}\right) q_2}{f_{01000}^{(2)} - iw_0},\ q_2 = \frac{iw_0 - f_{10}^{(1)}}{f_{01}^{(1)}},$$

$$q_1^* = -\frac{f_{10}^{(1)} + iw_0 + f_{010}^{(3)}\ e^{-i\tau_0 w_0} q_2^*}{f_{10000}^{(2)} + f_{00010}^{(2)}\ e^{-i\tau_0 w_0}},$$

$$q_2^* = \frac{f_{01}^{(1)}\left[f_{10000}^{(2)} + f_{00010}^{(2)}\ e^{-i\tau_0 w_0}\right] - \left[f_{00100}^{(2)} + f_{00001}^{(2)}\ e^{-i\tau_0 w_0}\right]\left[f_{10}^{(1)} + iw_0\right]}{\left[f_{00100}^{(2)} + f_{00001}^{(2)}\ e^{-i\tau_0 w_0}\right]\left[f_{010}^{(3)} e^{-i\tau_0 w_0} - f_{100}^{3} - f_{001}^{(3)}\ e^{-i\tau_0 w_0} - iw_0\right]}.$$

From bilinear inner product (28), we get:

$$\begin{aligned} \langle q^*(S), q(\theta) \rangle = \bar{D} \Big[ 1 + \bar{q}_1^* q_1 + \bar{q}_2^* q_2 + \bar{q}_1^* \tau_0 e^{-iw_0\tau_0} \left( f_{00010}^{(2)} + f_{00001}^{(2)} q_2 \right) \\ + \bar{q}_2^* \tau_0 e^{-iw_0\tau_0} \left( f_{010}^{(3)} + f_{001}^{(3)} q_2 \right) \Big]. \end{aligned} \tag{29}$$

Let, $D = \left[ 1 + q_1^* \bar{q}_1 + q_2^* \bar{q}_2 + \tau_0\ e^{-iw_0\tau_0} \left[ q_1^* \left( f_{00010}^{(2)} + f_{00001}^{(2)} \bar{q}_2 \right) + q_2^* \left( f_{010}^{(3)} + f_{001}^{(3)} \bar{q}_2 \right) \right] \right]^{-1}$,

where, $\bar{D}$ is the conjugate complex number of $D$, then $\langle q^*, q \rangle = 1$ and $\langle q^*, \bar{q} \rangle = 0$.

In the following, using similar arguments as in [31], it can be determined the properties of the Hopf

bifurcation:

$$\left.\begin{aligned} g_{20} &= 2\tau_0\bar{D}(L_1 + L_5\bar{q}_1^* + L_9\bar{q}_2^*) \\ g_{11} &= \tau_0\bar{D}(L_2 + L_6\bar{q}_1^* + L_{10}\bar{q}_2^*) \\ g_{02} &= 2\tau_0\bar{D}(L_3 + L_7\bar{q}_1^* + L_{11}\bar{q}_2^*) \\ g_{21} &= 2\tau_0\bar{D}(L_4 + L_8\bar{q}_1^* + L_{12}\bar{q}_2^*) \end{aligned}\right\} \tag{30}$$

where

$$L_1 = f_{11}^{(1)}\ q_2 + f_{02}^{(1)}\ q_2^2,$$

$$L_2 = f_{11}^{(1)}\ (q_1 + \bar{q}_2) + 2f_{02}^{(1)}\ q_2\bar{q}_2,$$

$$L_3 = f_{11}^{(1)}\ q_2 + f_{02}^{(1)}\ q_2^2,$$

$$L_4 = f_{11}^{(1)}\Big(\ q_2 + w_{11}^{(1)}(0) + \tfrac{1}{2}\ \bar{q}_2\ w_{20}^{(1)}(0) + \tfrac{1}{2}\ w_{20}^{(3)}(0) + w_{11}^{(3)}(0)\Big) + f_{02}^{(1)}\Big(\bar{q}_2\ w_{20}^{(3)}(0) + 2q_2\ w_{11}^{(3)}(0)\Big),$$

$$L_5 = f_{10100}^{(2)}\ q_2 + f_{00200}^{(2)}\ q_2^{(2)} + f_{00002}\ q_2^{(2)}\ e^{-2iw_0\tau_0},$$

$$L_6 = f_{10100}^{(2)}(q_2 + \bar{q}_2) + 2f_{00200}^{(2)}\ q_2\bar{q}_2 + 2f_{00002}^{(2)}\ q_2^2\ e^{-2iw_0\tau_0},$$

$$L_7 = f_{10100}^{(2)}\ \bar{q}_2 + f_{00200}^{(2)}\ \bar{q}_2 + f_{00002}\ \bar{q}_2^2\ e^{2iw_0\tau_0},$$

$$L_8 = f_{10100}^{(2)}\Big(\ q_2 + w_{11}^{(1)}(0) + \tfrac{1}{2}\bar{q}_2\ w_{20}^{(1)}(0) + \tfrac{1}{2}w_{20}^{(3)}(0) + w_{11}^{(3)}(0)\Big) + f_{00200}^{(2)}\Big(\bar{q}_2\ w_{20}^{(3)}(0) + 2q_2\ w_{11}^{(3)}(0)\Big) + f_{00002}^{(2)}\Big(\bar{q}_2\ w_{20}^{(3)}(-1)\ e^{iw_0\tau_0} + q_2\ w_{11}^{(3)}(-1)\ e^{-iw_0\tau_0}\Big),$$

$$L_9 = f_{011}^{(3)}\ q_2\ e^{-2iw_0\tau_0} + f_{200}^{(3)}\ q_2^2 + f_{002}^{(3)}\ q_2^2\ e^{-2iw_0\tau_0},$$

$$L_{10} = f_{011}^{(3)}(q_2 + \bar{q}_2) + 2f_{200}\ q_2\ \bar{q}_2 + 2f_{002}\ q_2\ \bar{q}_2,$$

$$L_{11} = f_{011}^{(3)}\ \bar{q}_2\ e^{2iw_0\tau_0} + f_{200}^{(3)}\ \bar{q}_2^2 + f_{002}^{(3)}\ \bar{q}_2^2\ e^{2iw_0\tau_0},$$

$$L_{12} = f_{011}^{(3)}\Big(\ q_2\ w_{11}^{(1)}(-1)\ e^{-iw_0\tau_0} + \tfrac{1}{2}\bar{q}_2\ w_{20}^{(1)}(-1)\ e^{iw_0\tau_0} + w_{11}^{(3)}(-1)e^{-iw_0\tau_0} + \tfrac{1}{2}\ w_{20}^{(3)}(-1)\ e^{iw_0\tau_0}\Big) + f_{200}^{(3)}\Big(\bar{q}_2\ w_{20}^{(3)}(0) + 2q_2\ w_{11}^{(3)}(0)\Big) + f_{002}^{(3)}\Big(\bar{q}_2\ w_{20}^{(3)}(-1)\ e^{iw_0\tau_0} + q_2\ w_{11}^{(3)}(-1)\ e^{-iw_0\tau_0}\Big).$$

with

$$w_{20}(\theta) = \frac{ig_{20}}{w_0\tau_0}\ q(0)\ e^{iw_0\tau_0\theta} + \frac{i\bar{g}_{02}}{3w_0\tau_0}\ \bar{q}(0)\ e^{-iw_0\tau_0\theta} + E_1\ e^{2iw_0\tau\theta}. \quad (31)$$

$$w_{11}(\theta) = -\frac{ig_{11}}{w_0\tau_0}\ q(0)\ e^{iw_0\tau_0\theta} + \frac{i\bar{g}_{11}}{w_0\tau_0}\bar{q}(0)\ e^{-iw_0\tau_0\theta} + E_2. \quad (32)$$

Notice that, $E_1 = \left(E_1^{(1)}, E_1^{(2)}, E_1^{(3)}\right)^T$ and $E_2 = \left(E_2^{(1)}, E_2^{(2)}, E_2^{(3)}\right)^T$ can be determined from the following equations:

$$J_1^*\ E_1 = 2\tau_0 J_1. \quad (33)$$

$$J_2^*\ E_2 = -\tau_0 J_2. \quad (34)$$

where

$$J_1^* = \left(2iw_0\tau_0 I - \int_{-1}^{0} d\psi(\theta)\ e^{2iw_0\tau_0\theta}\right),$$

$$J_2^* = \left(\int_{-1}^{0} d\psi(\theta)\right),$$

$$J_1 = (L_1\ \ L_5\ \ L_9)^T,$$

$$J_2 = (L_2\ \ L_6\ \ L_{10})^T.$$

Accordingly, it is obtained that:

$$J_1^* = \begin{pmatrix} 2iw_0 - f_{10}^{(1)} & 0 & -f_{01}^{(1)} \\ -f_{10000}^{(2)} - f_{00010}^{(2)}e^{-2iw_0\tau_0\theta} & 2iw_0 - f_{01000}^{(2)} & -f_{00100}^{(2)} - f_{00001}^{(2)}e^{-2iw_0\tau_0\theta} \\ -f_{010}^{(3)}\ e^{-2iw_0\tau_0\theta} & 0 & 2iw_0 - f_{100}^{(3)} - f_{001}^{(3)}e^{-2iw_0\tau_0\theta} \end{pmatrix}.$$

$$J_2^* = \begin{pmatrix} -f_{10}^{(1)} & 0 & -f_{01}^{(1)} \\ -f_{10000}^{(2)} - f_{00010}^{(2)} & -f_{01000}^{(2)} & -f_{00100}^{(2)} - f_{00001}^{(2)} \\ -f_{010} & 0 & -f_{100}^{(3)} - f_{001}^{(3)} \end{pmatrix}.$$

Thus, $E_1^{(i)} = \frac{2\triangle_i}{\triangle}, i = 1,2,3$, where $\triangle = Det\ (J_1^*)$ and $\triangle_i$ is the value of the determinant $V_i$, where $V_i$ is formed by replacing the $i^{th}$ column vector of $J_1^*$ by $J_1$ for $i = 1,2,3$. Similarly, $E_2^{(i)} = \frac{2\bar{\triangle}_i}{\bar{\triangle}}, i = 1,2,3$, where $\bar{\triangle} = Det\ (J_2^*)$ and $\bar{\triangle}_i$ is the value of the determinant $U_i$, where $U_i$ is formed by replacing the $i^{th}$ column vector of $J_2^*$ by $J_2$ for $i = 1,2,3$.

Consequently, $w_{20}(\theta)$ and $w_{11}(\theta)$ can be computed using equations (31)-(34). Then the

expressions given in equation (19) can be determined depending on those given in equation (30) and the proof is done.

## 9. THE NUMERICAL SIMULATIONS

The objectives of this section are to determine the effect of changing parameter values and to corroborate our analytical conclusions from previous sections by employing a standard MATLAB algorithm with different physiologically plausible sets of hypothetical parameter values as shown in Eq. (35) and Eq. (36) respectively.

$$\Lambda = 3, \beta_1 = 0.055, \beta_2 = 0.0001, \mu = 0.3, m = 10, \alpha = 0.0001, \\ k = 0.1, \gamma = 0.01, a = 0.25, b = 0.1, \tau = 2 \tag{35}$$

and

$$\Lambda = 5, \beta_1 = 0.05, \beta_2 = 0.01, \mu = 0.05, m = 10, \alpha = 0.1, \\ k = 0.1, \gamma = 0.18, a = 0.1, b = 0.3, \tau = 2 \tag{36}$$

To explore the influence of changing one or more parameter values at a time on the dynamical behavior of model (2), the following results were obtained:

1. The requirement of theorem 3 is satisfied for parameters in the set (35), i.e. $R_0 = 0.97 < 1$. In this scenario, the system (2)'s DFEP that is given by $Q_0(10, 0)$ is locally asymptotically stable (see Figure 2).
2. The condition of theorem 5 is satisfied, for parameters in the set (35) with $\beta_1 = 0.09$, i.e. $R_0 = 1.59 > 1$. Then the EEP that is given by $Q^*(8.71, 0.49)$ is a globally asymptotically stable (see Figure 3).
3. The dynamic behavior of the system (2) is unaffected qualitatively by changing the parameter values $(\gamma . k)$ that is, the system still approaches an endemic equilibrium point.
4. On the other hand, for the set of data (36), it is observed that system (2) approaches $Q^*(59.2,6.67)$ and $R_0 = 19.67 > 1$, starting from different initial sets of points (see Figure 4).
5. Figure 5 shows the impact of altering $\beta_1$ on the infected population $I(t)$, keeping the rest of parameters as in set (36). It was discovered that they have a positive proportionality. In

contrast, as illustrated in Figure 6, there is a negative proportionality between the $\alpha$ rate and the infected population.

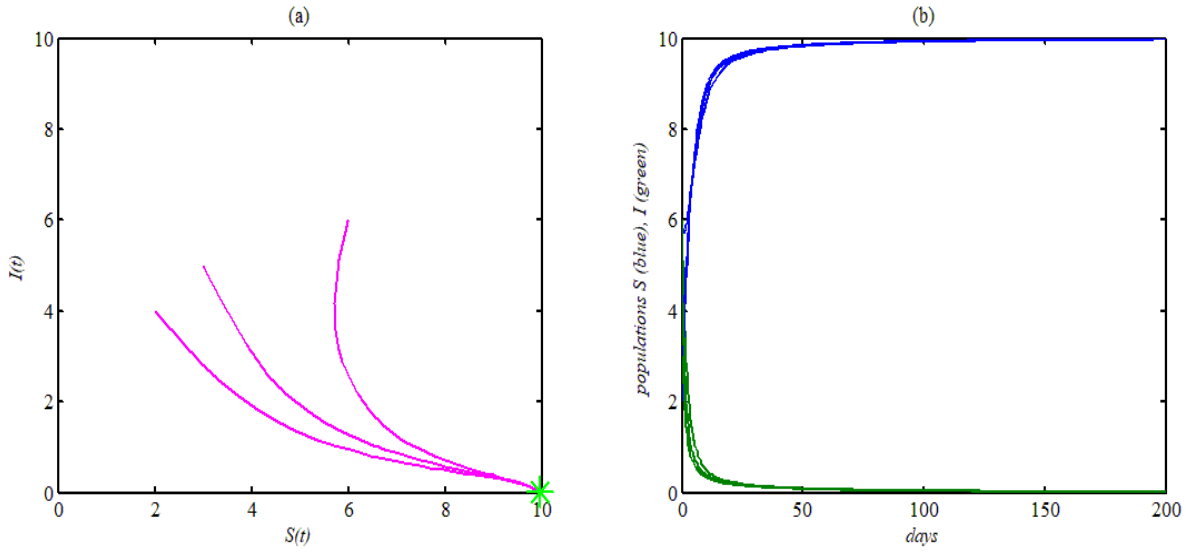


**Figure 2**: The solution of the system (2) for the parameters set (35) starting from different initial points. (a) A globally asymptotically stable DFEP in the $SI$ −plane. (b) Time series of (a).

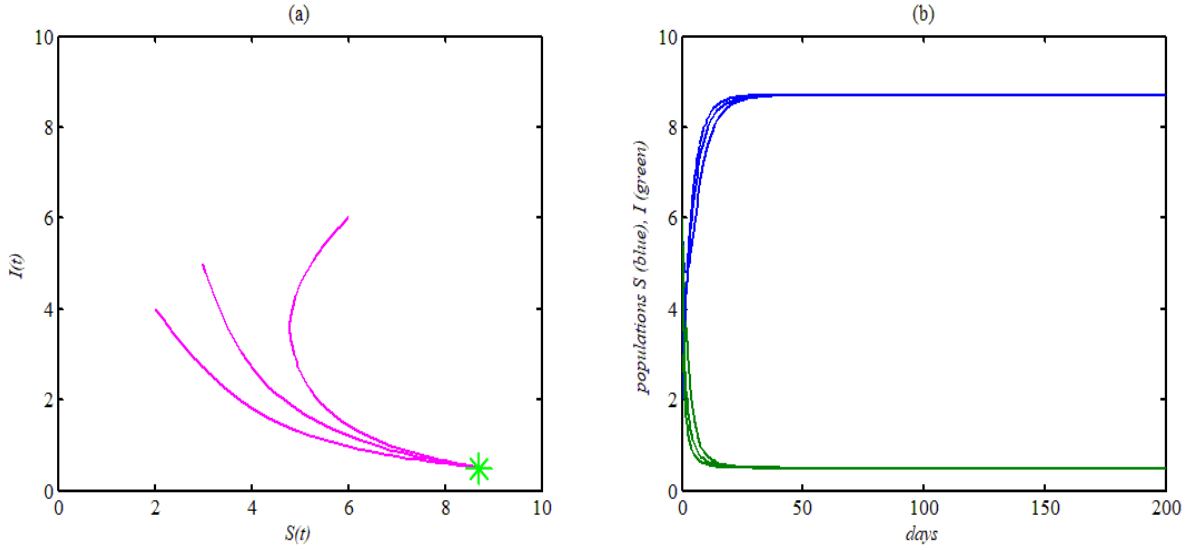


**Figure 3**: The solution of the system (2) for the parameters set (35) with $\beta_1 = 0.09$ starting from different initial points. (a) A globally asymptotically stable EEP in the $SI$ −plane. (b) Time series of (a).

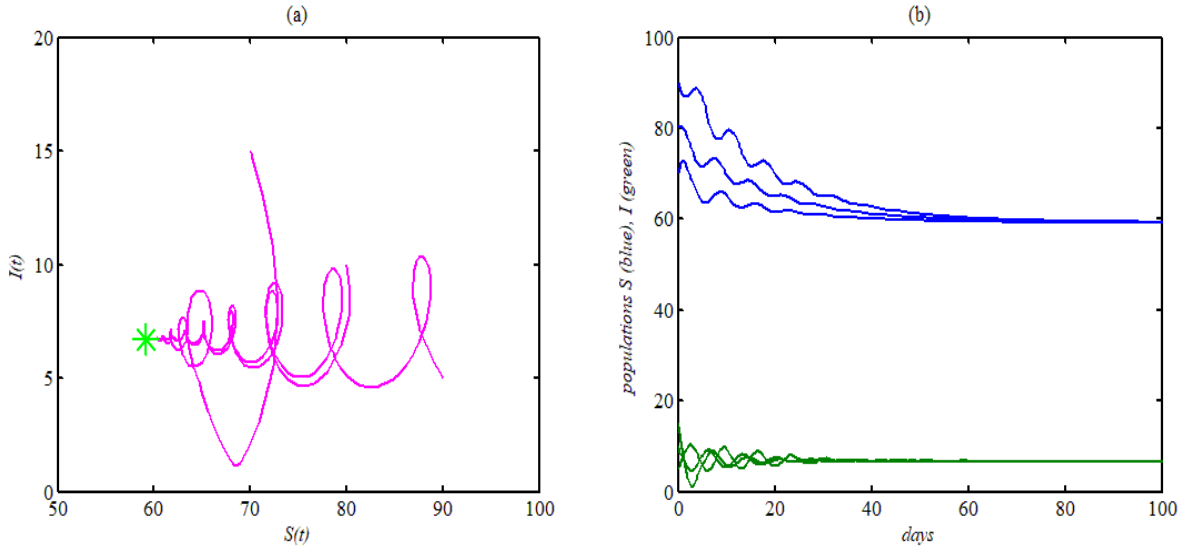


**Figure 4**: The solution of the system (2) for the parameters set (36) starting from different initial points. (a) A globally asymptotically stable EEP in the $SI$ −plane. (b) Time series of (a).

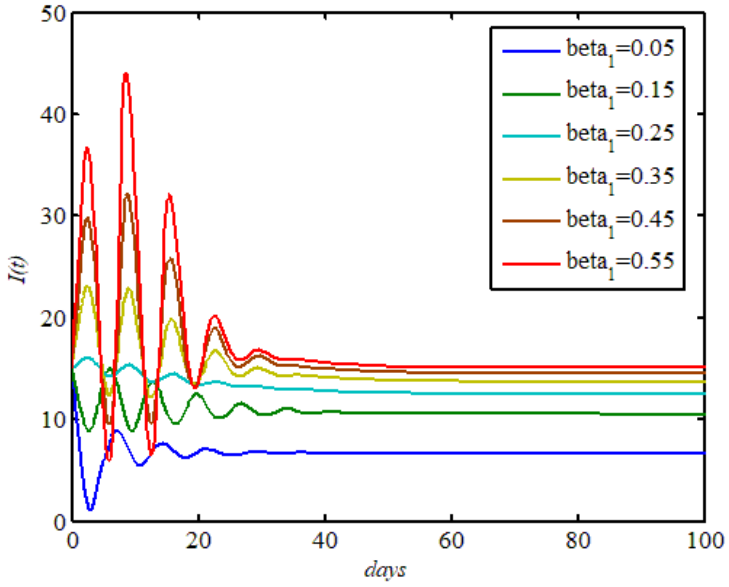


**Figure 5**: The infected trajectory of the system (2) as a function of time for the parameters set (36) with different values of $\beta_1$.

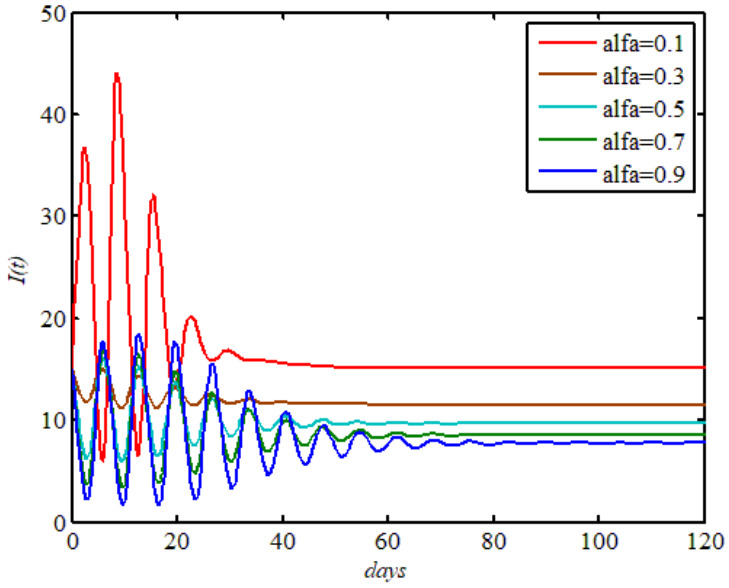


**Figure 6**: The infected trajectory of the system (2) as a function of time for the parameters set (36) with $\beta_1 = 0.55$ and different values of $\alpha$.

6. Figure 7 shows the impact of altering $a$ on the infected population $I(t)$, keeping the rest of parameters as in set (36). It was discovered that they have a negative proportionality. In contrast, as illustrated in Figure 8, there is a positive proportionality between the $b$ rate and the infected population.
7. The impact of varying $\alpha$ and/or $a$, on the infected population, keeping the rest of parameters as in set (36), is investigated in Figure 9. It is observed that increasing both of them decreases the infected population.
8. The impact of varying $m$, on the infected population, keeping the rest of parameters as in set (36), is investigated in Figure 10. It is observed that they have a positive proportionality.
9. The impact of varying $\mu$, on the infected population, keeping the rest of parameters as in set (36), is investigated in Figure 11. It is observed that they have a negative proportionality.
10. Now, the requirements of the theorem 6 is satisfied for parameters in the set (36) with $\tau_0 = 4.1$, as shown in the figures 12,13, and 14. It is observed that for $\tau < \tau_0$, the EEP is asymptotic stable. However, for $\tau > \tau_0$, the EEP becomes unstable and a Hopf bifurcation occurs with an increasing period as $\tau$ increases.

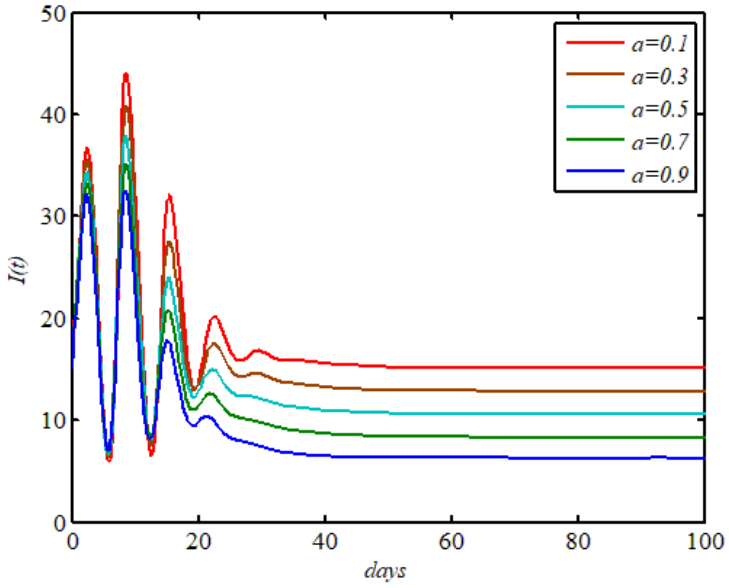


**Figure 7**: The infected trajectory of the system (2) as a function of time for the parameters set (36) with $\beta_1 = 0.55$ and different values of $a$.

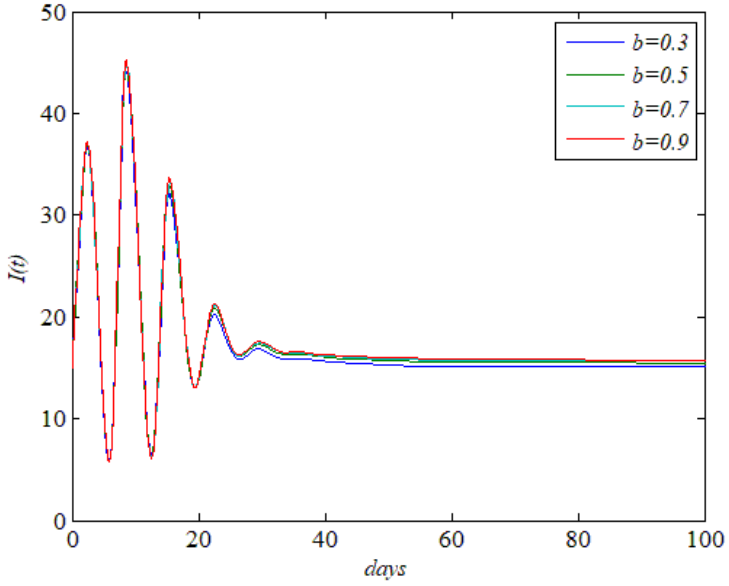


**Figure 8**: The infected trajectory of the system (2) as a function of time for the parameters set (36) with $\beta_1 = 0.55$ and different values of $b$.

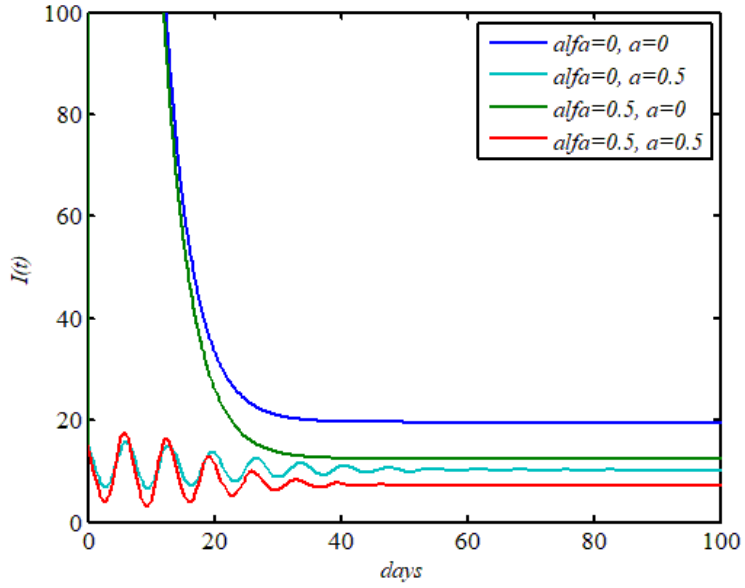


**Figure 9**: The infected trajectory of the system (2) as a function of time for the parameters set (36) with $\beta_1 = 0.55$ and different values of $\alpha$, and $a$.

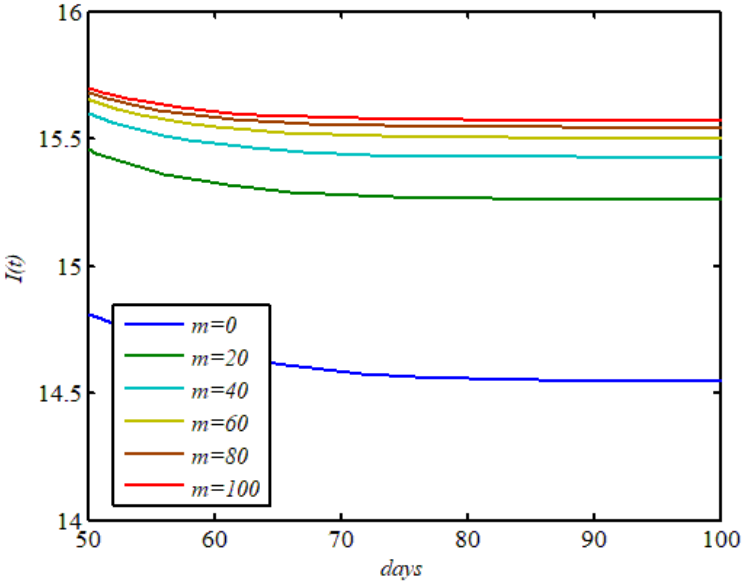


**Figure 10**: The infected trajectory of the system (2) as a function of time for the parameters set (36) with $\beta_1 = 0.55$ and different values of $m$.

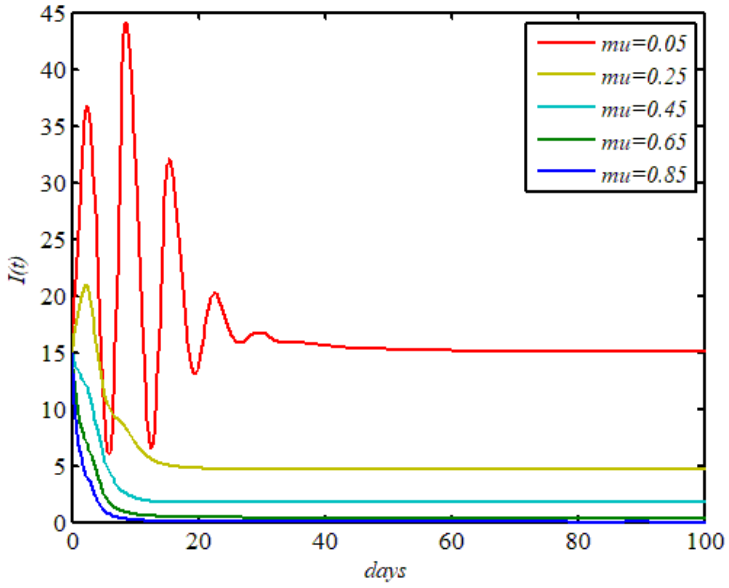


**Figure 11**: The infected trajectory of the system (2) as a function of time for the parameters set (36) with $\beta_1 = 0.55$ and different values of $\mu$.

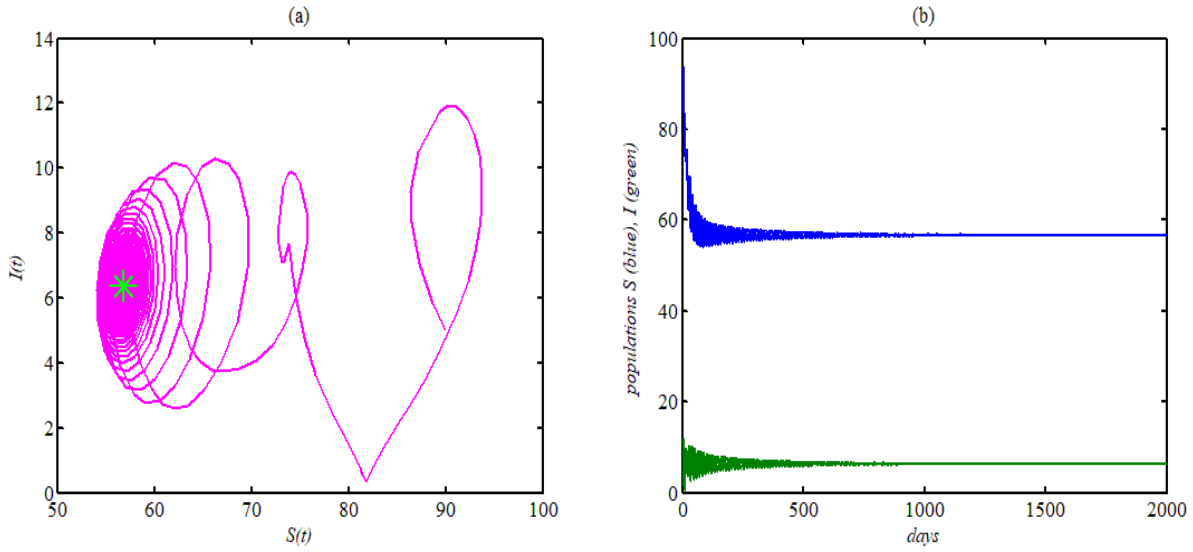


**Figure 12**: The solution of the system (2) for the parameters set (36) with $\mu = 4$. (a) A globally asymptotically stable EEP in the $SI$ −plane. (b) Time series of (a).

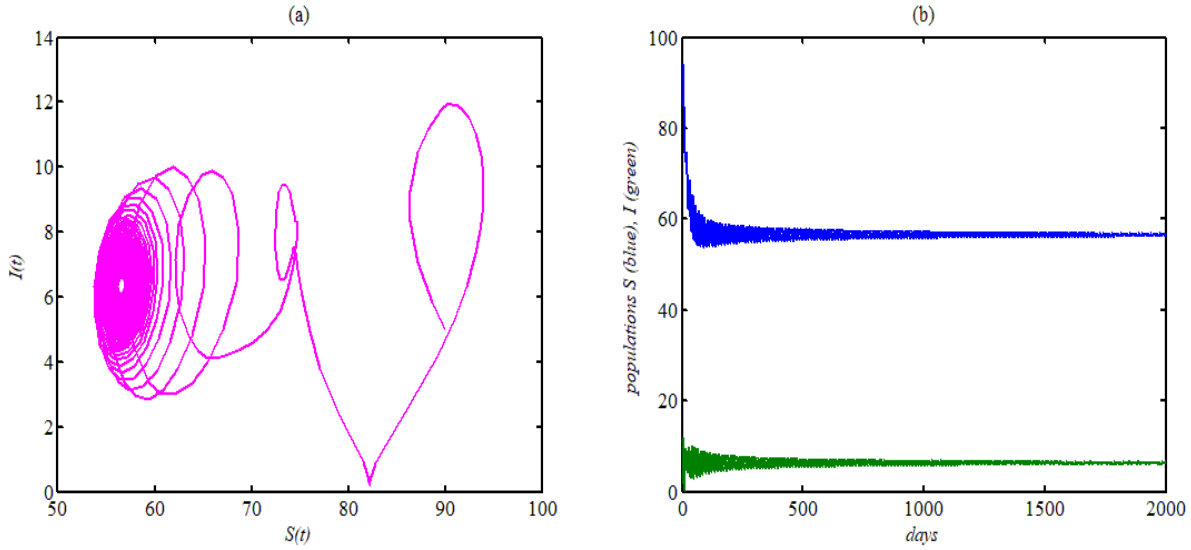


**Figure 13**: The solution of the system (2) for the parameters set (36) with $\mu = 4.1$. (a) Hopf bifurcation occurs in the $SI$ −plane with small period. (b) Time series of (a).

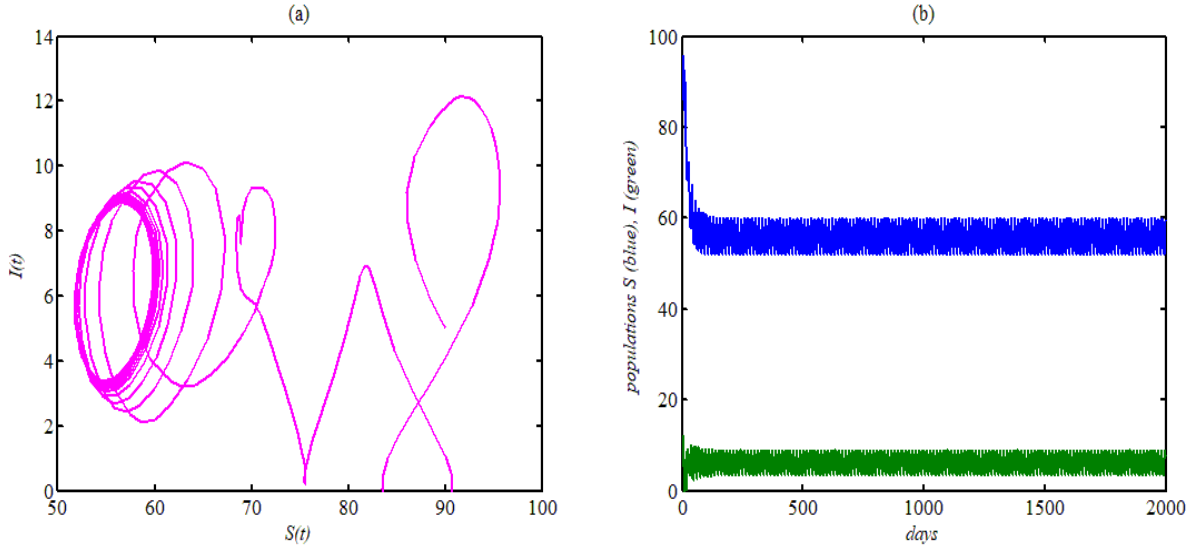


**Figure 14**: The solution of the system (2) for the parameters set (36) with $\mu = 5$. (a) Hopf bifurcation occurs in the $SI$ −plane with long period. (b) Time series of (a).

## 10. CONCLUSIONS

A delayed SEIR epidemic model is developed in this study so that it includes the effects of two nonlinear functions: the effect of media coverage on disease transmission and the effect of treatment rate on infection disease. The mathematical examination of the model reveals the

existence of two equilibria, the DFEP, and the EEP. The local and global asymptotic stability of DFEP and EEP, respectively, is investigated by establishing the basic reproduction number $R_0$. It is obtained $R_0 < 1$ implies that the disease can be eradicated from society, whereas $R_0 > 1$ implies that it will persist. Assumptions (H1)–(H6) are provided to obtain the global stability of the equilibrium points of system (2). It has been demonstrated that the EEP is asymptotically stable for $R_0 > 1$ when the delay $\tau$ does not reach a particular value $\tau_0$. However, for $\tau > \tau_0$, it becomes the unstable point, and a Hopf bifurcation occurs. The center manifold technique in the sense of Hassard is used to study all of the properties of the Hopf bifurcation theoretically. Finally, the global dynamics of the system (2) are numerically explored using Matlab version 2013 for various sets of parameters and initial points. The following are the outcomes.

The system (2) has two equilibrium points: the FDEP and EEP, which are a globally asymptotically stable for different sets of parameters provided that $R_0 < 1$ and $R_0 > 1$ respectively. Moreover, the EEP becomes unstable and the solution approaches asymptotically to periodic dynamics due to Hopf bifurcation when $\tau > \tau_0$. The infected population is proportional positively to changing the contact rate before the media coverage alert while retaining the rest of the parameters as in set (36). The inhibitory impact rate and the infected population, on the other hand, have a negative proportionality. The infected population is proportional positively to changing the limitation rate while retaining the rest of the parameters as in set (36). The cure rate and the infected population, on the other hand, have a negative proportionality. The infected population is proportional positively to changing the non-response rate of individuals to media coverage while retaining the rest of the parameters as in set (36). The natural death rate and the infected population, on the other hand, have a negative proportionality. Finally, the infected population is proportional negatively to changing the inhibitory effect and / or cure rate while retaining the rest of the parameters as in set (36).

## CONFLICT OF INTERESTS

The author(s) declare that there is no conflict of interests.

## REFERENCES

[1] R.K. Naji, R.M. Hussien, The dynamics of epidemic model with two types of infectious diseases and vertical transmission, J. Appl. Math. 2016 (2016), 4907964. https://doi.org/10.1155/2016/4907964.

[2] C.J.E. Metcalf, D.H. Morris, S.W. Park, Mathematical models to guide pandemic response, Science. 369 (2020), 368–369. https://doi.org/10.1126/science.abd1668.

[3] A.A. Mohsen, H.F. Al-Husseiny, K. Hattaf, The awareness effect of the dynamical behavior of sis epidemic model with Crowley-martin incidence rate and Holling type III treatment function, Int. J. Nonlinear Anal. Appl. 12 (2021), 1083–1097.

[4] F. Brauer, P. van den Driessche, J. Wu, eds., Mathematical epidemiology, Springer Berlin Heidelberg, Berlin, Heidelberg, 2008. https://doi.org/10.1007/978-3-540-78911-6.

[5] M. Lu, J. Huang, S. Ruan, P. Yu, Bifurcation analysis of an SIRS epidemic model with a generalized nonmonotone and saturated incidence rate, J. Differ. Equ. 267 (2019), 1859–1898. https://doi.org/10.1016/j.jde.2019.03.005.

[6] A.K.S. Al-Tameemi, R.K. Naji, The impact of media coverage and curfew on the outbreak of coronavirus disease 2019 model: Stability and bifurcation, Int. J. Differ. Equ. 2021 (2021), 1892827. https://doi.org/10.1155/2021/1892827.

[7] M. Banerjee, A. Tokarev, V. Volpert, Immuno-epidemiological model of two-stage epidemic growth, Math. Model. Nat. Phenom. 15 (2020), 27. https://doi.org/10.1051/mmnp/2020012.

[8] M.Y. Li, J.S. Muldowney, Global stability for the SEIR model in epidemiology, Math. Biosci. 125 (1995), 155–164. https://doi.org/10.1016/0025-5564(95)92756-5.

[9] K. Prem, Y. Liu, T.W. Russell, et al. The effect of control strategies to reduce social mixing on outcomes of the COVID-19 epidemic in Wuhan, China: a modelling study, The Lancet Public Health. 5 (2020), e261–e270. https://doi.org/10.1016/s2468-2667(20)30073-6.

[10] F. Yang, S.C.A. Nielsen, R.A. Hoh, et al. Shared B cell memory to coronaviruses and other pathogens varies in human age groups and tissues, Science. 372 (2021), 738–741. https://doi.org/10.1126/science.abf6648.

[11] M. Chinazzi, J.T. Davis, M. Ajelli, et al. The effect of travel restrictions on the spread of the 2019 novel coronavirus (COVID-19) outbreak, Science. 368 (2020), 395–400. https://doi.org/10.1126/science.aba9757.

[12] X. Tan, L. Yuan, J. Zhou, Y. Zheng, F. Yang, Modeling the initial transmission dynamics of influenza A H1N1 in Guangdong Province, China, Int. J. Infect. Dis. 17 (2013) e479–e484. https://doi.org/10.1016/j.ijid.2012.11.018.

[13] A. Svensson, A note on generation times in epidemic models, Math. Biosci. 208 (2007) 300–311. https://doi.org/10.1016/j.mbs.2006.10.010.

[14] X. Liu, L. Yang, Stability analysis of an SEIQV epidemic model with saturated incidence rate, Nonlinear Anal.: Real World Appl. 13 (2012), 2671–2679. https://doi.org/10.1016/j.nonrwa.2012.03.010.

[15] H. Abdul-Satar, R.K. Naji, Stability and bifurcation of a cholera epidemic model with saturated recovery rate, Appl. Appl. Math.: Int. J. 16 (2021), 27. https://digitalcommons.pvamu.edu/aam/vol16/iss2/27.

[16] A.A. Thirthar, R.K. Naji, F. Bozkurt, A. Yousef, Modeling and analysis of an $SI_1I_2R$ epidemic model with nonlinear incidence and general recovery functions of $I_1$, Chaos Solitons Fractals. 145 (2021), 110746. https://doi.org/10.1016/j.chaos.2021.110746.

[17] R. Xu, Y. Du, A delayed SIR epidemic model with saturation incidence and a constant infectious period, J. Appl. Math. Comput. 35 (2009), 229–250. https://doi.org/10.1007/s12190-009-0353-3.

[18] R. Xu, Z. Ma, Global stability of a delayed SEIRS epidemic model with saturation incidence rate, Nonlinear Dyn. 61 (2010), 229–239. https://doi.org/10.1007/s11071-009-9644-3.

[19] A. Kumar, Nilam, Mathematical analysis of a delayed epidemic model with nonlinear incidence and treatment rates, J. Eng. Math. 115 (2019), 1–20. https://doi.org/10.1007/s10665-019-09989-3.

[20] D. Xiao, S. Ruan, Global analysis of an epidemic model with nonmonotone incidence rate, Math. Biosci. 208 (2007), 419–429. https://doi.org/10.1016/j.mbs.2006.09.025.

[21] S. Ruan, W. Wang, Dynamical behavior of an epidemic model with a nonlinear incidence rate, J. Differ. Equ. 188 (2003), 135–163. https://doi.org/10.1016/s0022-0396(02)00089-x.

[22] J. Cui, Y. Sun, H. Zhu, The impact of media on the control of infectious diseases, J. Dyn. Differ. Equ. 20 (2007), 31–53. https://doi.org/10.1007/s10884-007-9075-0.

[23] Y. Liu, J.A. Cui, The impact of media coverage on the dynamics of infectious disease, Int. J. Biomath. 01 (2008), 65–74. https://doi.org/10.1142/s1793524508000023.

[24] Y. Xiao, T. Zhao, S. Tang, Dynamics of an infectious diseases with media/psychology induced non-smooth incidence, Math. Biosci. Eng. 10 (2013), 445–461. https://doi.org/10.3934/mbe.2013.10.445.

[25] J.M. Tchuenche, N. Dube, C.P. Bhunu, et al. The impact of media coverage on the transmission dynamics of human influenza, BMC Public Health. 11 (2011), S5. https://doi.org/10.1186/1471-2458-11-s1-s5.

[26] C. Sun, W. Yang, J. Arino, K. Khan, Effect of media-induced social distancing on disease transmission in a two patch setting, Math. Biosci. 230 (2011), 87–95. https://doi.org/10.1016/j.mbs.2011.01.005.

[27] W. Wang, S. Ruan, Bifurcations in an epidemic model with constant removal rate of the infectives, J. Math. Anal. Appl. 291 (2004), 775–793. https://doi.org/10.1016/j.jmaa.2003.11.043.

[28] L. Zhou, M. Fan, Dynamics of an SIR epidemic model with limited medical resources revisited, Nonlinear Anal.: Real World Appl. 13 (2012), 312–324. https://doi.org/10.1016/j.nonrwa.2011.07.036.

[29] B. Dubey, P. Dubey, U.S. Dubey, Dynamics of an sir model with nonlinear incidence and treatment rate, Appl. Appl. Math.: Int. J. 2 (2015), 718 – 737. https://digitalcommons.pvamu.edu/aam/vol10/iss2/5.

[30] L. Perko, Differential equations and dynamical systems, Springer Science & Business Media, New York, 2013.

[31] B.D. Hassard, N.D. Kazarinoff, Y.H. Wan, Theory and applications of hopf bifurcation, London Math. Soc. Lecture Notes 41. Cambridge University Press, 1981.